Stroke
JOURNAL OF THE AMERICAN HEART ASSOCIATION
American Stroke Association
A Division of American Heart Association

MRI Detection of Secondary Damage After Stroke: Chronic Iron Accumulation in the Thalamus of the Rat Brain

Carles Justicia, Pedro Ramos-Cabrer and Mathias Hoehn

Stroke 2008;39;1541-1547; originally published online Mar 6, 2008;
DOI: 10.1161/STROKEAHA.107.503565
Stroke is published by the American Heart Association. 7272 Greenville Avenue, Dallas, TX 72514
 Print ISSN: 0039-2499. Online ISSN: 1524-4628

MRI Detection of Secondary Damage After Stroke
Chronic Iron Accumulation in the Thalamus of the Rat Brain

Carles Justicia, PhD; Pedro Ramos-Cabrer, PhD; Mathias Hoehn, PhD

Background and Purpose—Iron plays a central role in many metabolic processes. Under certain pathological situations it accumulates, producing negative effects such as increasing damage by oxidative stress. The present study examined long-term iron accumulation in a stroke model with secondary degeneration, using MRI and histological techniques.

Methods—Male Wistar rats (n=22) were subjected to 60 minutes MCA occlusion. MR images (T2- and T2*-weighted) were obtained weekly between weeks 1 and 7 after reperfusion, and at weeks 10, 14, 20, and 24. Histological iron detection and immunohistochemical examination for different markers (NeuN, GFAP, OX-42, HO-1, and APP) were performed at the 3 survival time points (3, 7, and 24 weeks).

Results—Infarcts affecting MCA territory were evident on T2-weighted imaging, and all animals showed deficits on behavioral tests. In the thalamus, T2 hyperintensity was detected 3 weeks after stroke, and disappeared around week 7 when T2*-weighted images showed a marked hypointensity in that area. Histology revealed neuronal loss in the thalamus, accompanied by strong microglial reactivity and microglial HO-1 expression. APP deposits were detected in the thalamus from week 3 on and persisted until week 24. Iron storage was detected in microglia at week 3, in the parenchyma at week 7, and around APP deposits at week 24.

Conclusions—T2*-weighted MRI allows the detection of secondary damage in the thalamus after MCAO. Iron accumulation in the thalamus is mediated by HO-1 expression in reactive microglia. **(*Stroke*. 2008;39:1541-1547.)**

Key Words: transient cerebral ischemia ■ thalamus ■ magnetic resonance imaging ■ iron ■ heme-oxigenase-1

Reduction of regional cerebral blood flow may result in brain infarction. The most common experimental brain infarction model is the occlusion of the middle cerebral artery (MCAO), directly affecting ipsilateral cerebral cortex and caudate putamen. Focal brain ischemia also leads to changes in regions remote from the primary affected areas.[1,2] These changes include vasogenic edema[3,4] and excitotoxicity,[5–7] which can contribute to secondary damage early after the insult. Cerebral infarct is one of the most common causes of Wallerian anterograde degeneration. After proximal axonal or somal injury, a degeneration of axons and myelin sheaths is observed. This axonal degeneration and myelin clearance give rise to accumulation of proteins and ions in the distal affected regions,[8] contributing to the secondary lesion. Secondary damage also generates chronic microglial responses in the thalamus.[9,10]

Iron is essential for cell function and is involved in many important processes such as oxygen transport, storage, and activation. Iron storage is mediated by ferritin. High plasma ferritin levels have been related to poorer prognosis after stroke[11] because ferritin is a source of free iron. Accumulation of iron, after hypoxia/ischemia in newborns, can be detected with MRI techniques.[12] This iron accumulation causes pronounced susceptibility effects, thus reducing local T2 relaxation time, which results in hypointensity on T2*-weighted (T2*-W) images. High iron content of blood cells allows the detection of different events such as hemorrhages in the brain parenchyma and hemorrhagic transformation after brain infarct. Other pathologies, such as Alzheimer disease, can lead to iron accumulation in the brain. Different metal ions (iron, copper, zinc) have been found to accumulate around senile plaques.[13]

Heme-containing proteins are a source of iron during brain injury. Inducible heme oxygenase (HO-1) is a heat shock protein that responds to stress, catabolizing free heme into iron, carbon monoxide, and biliverdin (an antioxidant). Thus, HO-1 has been suggested to be protective against oxidative stress.[14]

The aim of this work was to study, by MRI techniques, the different events taking place during and after thalamic secondary degeneration. Our hypothesis was that HO-1, transiently expressed by reactive microglia in the thalamus, contributes to chronic iron accumulation in the thalamus and is detectable by MRI.

Received August 31, 2007; final revision received October 1, 2007; accepted October 3, 2007.

From the In-vivo-NMR-Laboratory (C.J., P.R.-C., M.H.), Max Planck Institute for Neurological Research, Cologne, Germany; Brain Ischemia and Neurodegeneration (C.J.), IIBB-CSIC, IDIBAPS, Barcelona, Spain; and Clinical Neurosciences Research Laboratory (P.R.-C.), Hospital Clínico Universitario, Santiago de Compostela, Spain.

Correspondence to Prof Dr Mathias Hoehn, In-vivo-NMR-Laboratory, Max-Planck-Institute for Neurological Research, Gleuelerstrasse 50, D-50931 Cologne, Germany. E-mail mathias@nf.mpg.de

Stroke **is available at http://stroke.ahajournals.org** **DOI: 10.1161/STROKEAHA.107.503565**

Materials and Methods

Animals

Male Wistar rats (n=22; 280 to 320 g body weight at the beginning of the study; Harlan; Borschen, Germany) were used for the longitudinal study of secondary degeneration after stroke. One animal with abnormal T2* MRI before stroke induction was excluded from the study. Rats were euthanized at 3 different survival time points: 3 weeks (n=5), 7 weeks (n=8), and 24 weeks (n=8). All experiments were performed in accordance with the National Institute of Health animal protection guidelines and approved by the local governmental authorities.

Induction of Ischemia

Focal cerebral ischemia was produced by 1-hour intraluminal occlusion of MCA followed by reperfusion. Rats were kept under 1 to 1.5% halothane in nitrous oxide/oxygen (70:30) during all surgical procedures. The right common carotid artery was exposed, and branches of the external carotid artery (ECA) were electrocoagulated and sectioned. The pterygopalatine artery was tied close to the internal carotid artery. The common carotid artery was permanently occluded with a silk thread (3/0). A filament (4/0 Ethicon sutures), coated with silicon, was introduced through the ECA to the level of the MCA branching point. During MCAO rats showed a decrease in cortical blood flow measured by LDF with normal blood flow recovery after reperfusion. All animals showed infarction in the right parietal cortex and caudate-putamen (MCA territory) on T2-weighted MRI at 48 hours after stroke induction. Other brain regions, irrigated by anterior and posterior cerebral arteries, were not affected.

Adhesive Removal Test

Somatosensory deficits were assessed with the adhesive removal test. Experiments were done during the dark part of the day/night cycle, when animals show higher activity. The adhesive removal test was performed as described by Schallert and colleagues[15] and applied in our laboratory.[16] Briefly, 2 adhesive paper dots (12 mm diameter) were accurately attached to the distal-radial region on the wrist of each forelimb. Both the time to contact each paw and the time to remove paper dots were recorded 3 times, with a minimal interval of 5 minutes between consecutive trials. Before the first (preischemic) MRI session animals were trained for 3 consecutive days. Tests were always carried out the day before each MRI experiment.

MRI

MRI experiments were conducted on 4.7 T and 7 T horizontal bore magnets (Bruker BioSpin, Germany) with 20-cm wide actively shielded gradient coils (100 and 200 mT/m, respectively). Radiofrequency transmission was achieved with home-built Helmholtz coils (12 cm diameter); signal was detected using 2.2 cm surface coils, positioned over the head of the animal, which was fixed with tooth bar, ear plugs, and adhesive tape. Transmission and reception rf coils were actively decoupled from each other. Gradient-echo pilot scans were performed at the beginning of each imaging session for accurate positioning of the animal inside the magnet bore. T2-weighted (T2-W) images were acquired using a multi-slice multi-echo spin-echo sequence with the following acquisition parameters: field-of-view=3.2×3.2 cm^2, image matrix=128×128 (isotropic in-plane resolution of 250 μm), 16 consecutive slices of 1 mm thickness, repetition time TR=3 seconds, 16 echoes with echo time TE of 7.5 ms (7T) or 12 ms (4.7T). T2*-weighted 3D data sets were acquired only at 4.7 T (to take advantage of the shorter T1 values at lower field) using gradient-echo sequence with the following acquisition parameters: field-of-view=2.0×2.0×1.0 cm^3, image matrix=160×160×40 (zero-filled to 256×256×64, spatial resolution: 78×78×156 μm), TR/TE=200/20 ms, excitation pulse angle=30°. All images were processed using ImageJ (Rasband, W.S., ImageJ, NIH, http://rsb.info.nih.gov/ij).

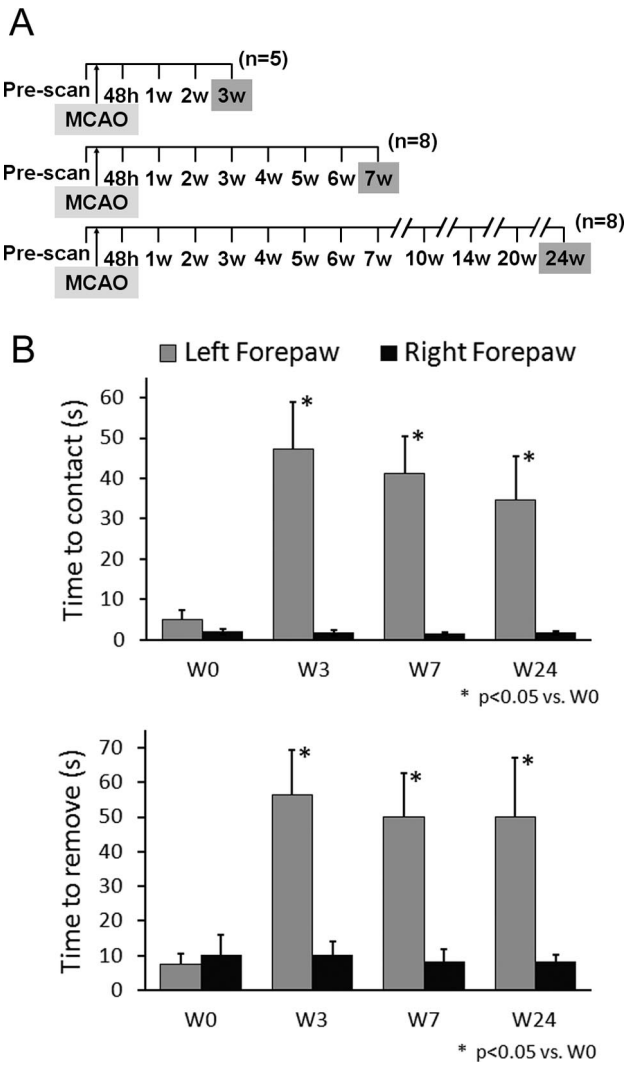

Figure 1. A, Experimental design indicating 3 animal groups with different survival times: 3 weeks, 7 weeks, and 24 weeks after MCAO. At every indicated time point behavioral tests and MRI were performed followed by histology/immunohistochemistry at the end of the survival period. B, Sticky tape removal test. Time to contact and time to remove the adhesive dots showed no differences between left and right forepaw before MCAO (W0). Delays in time to contact and to remove the tape indicate the corticostriatal damage caused by MCAO. Animals showed a slight tendency to improve long time after stroke.

Immunohistochemistry

Brains of all animals were processed for histological procedures. Expression of HO-1 and APP (Amyloid Precursor Protein) and identification of neurons, astrocytes, and microglia was performed by immunohistochemistry. Rats were perfused with 0.1 mol/L sodium phosphate buffer (PBS) pH 7.2, followed by 4% paraformaldehyde in the same buffer. Brains were postfixed overnight with the same fixative at 4°C and cryoprotected in 30% sucrose solution for 3 days. 40-μm-thick coronal sections were cut with a freezing microtome (Leica, Nussloch, Germany) and stored in a cryoprotectant solution. Free-floating sections were used for immunohistochemical detection for neurons, glial cells, inducible heme-oxygenase, and amyloid precursor protein.

Endogenous peroxidases were blocked with methanol-H_2O_2 and unspecific-binding sites with 3% normal horse serum for 2 hours at room temperature. Sections were incubated at 4°C with a mouse monoclonal antibody against either NeuN (neuronal marker; Chemicon Int, diluted 1:400), GFAP (astrocyte marker; Advanced Immu-

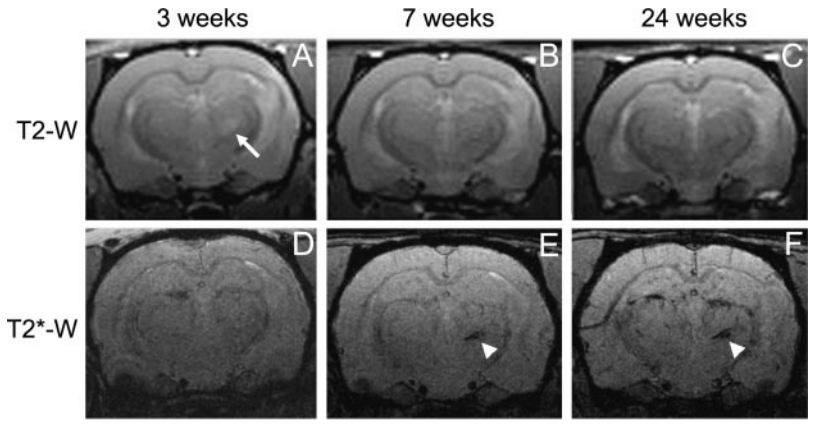

Figure 2. Successive changes of T2- and T2*-weighted MR images in the same rat after 60-minute MCAO. T2-W images (second echo, TE=15 ms) showed a transient hyperintensity, suggestive of edema in the right ipsilateral thalamus 3 weeks after ischemia (arrow in A), whereas this hyperintensity had disappeared at 7 weeks (B, C). 3D T2*-weighted images were acquired at the same MR sessions, showing a persistent hypointensity (arrowheads in E and F) in the thalamus from week 7 until the end of the experiment (24 weeks).

nochemicals Inc, diluted 1:400), OX42 (microglial marker; Stressgen, diluted 1:500), HO-1 (Chemicon Int, diluted 1:500), and APP (Chemicon Int, diluted 1:400). This was followed by biotinylated goat antimouse antibody (Vectastain, Vector) diluted 1:200 for 1 hour at room temperature and the avidin-biotin complex (ABC kit, Vector Laboratories; 1:100) for 1 hour. The reaction was developed with 0.05% diaminobenzidine and 0.03% H_2O_2.

Double immunohistochemistry was carried out after the first immunoreaction with OX42 or APP. The second primary antibodies were: a mouse monoclonal antibody against HO-1 (diluted 1:500) and a mouse monoclonal antibody against OX42 (diluted 1:500). Sections previously reacted with the first primary antibody were incubated with the second primary antibody, followed by a corresponding biotinylated secondary antibody. All sections were then incubated with the avidin-biotin complex, washed with 0.01 mol/L sodium phosphate buffer (pH 6), and preincubated for 10 minutes with 0.01% benzidine dihydrochloride and 0.025% sodium nitroferricyanide in 0.01 mol/L sodium phosphate buffer (pH 6). The reaction was developed with this solution containing 0.005% H_2O_2. All sections were mounted, dehydrated, and coverslipped with mounting medium (Enthelan, Fluka).

Images were acquired using Leica MZ FL III and Leica DM RB light microscopes, both equipped with a CCD camera.

Pearl Prussian Blue Staining

Coronal sections (40 μm) from all animals were processed for iron detection. Sections were mounted on glass slides. Hydrochloric acid (2%) and potassium hexacyanoferrat (2%) were mixed just before use (working solution). Sections were rinsed in working solution for 20 minutes. After washing in distilled water sections were either counterstained with nuclear fast red or processed for OX42 immunostaining.

Image Analysis

Infarct volume was determined from quantitative T2 maps recorded at 3 weeks after stroke. Lesion volume was defined as an increase of T2 by more than 2 standard deviations above the homotopic contralateral values.

Statistical Analysis

The statistical comparison of lesion volumes at 3 weeks after stroke and of response times of the behavioral test was performed for all studied animals at weeks 3, 7, and 24 using Student *t* test. A probability value of <0.05 was considered significant.

Results

Figure 1A shows the experimental design. Behavioral tests indicated significant differences between healthy and impaired hemispheres. Time-to-contact and time-to-remove (Figure 1B) the sticky tape increased dramatically on the left forepaw (contralateral to the lesion), whereas the right forepaw did not express significant changes.

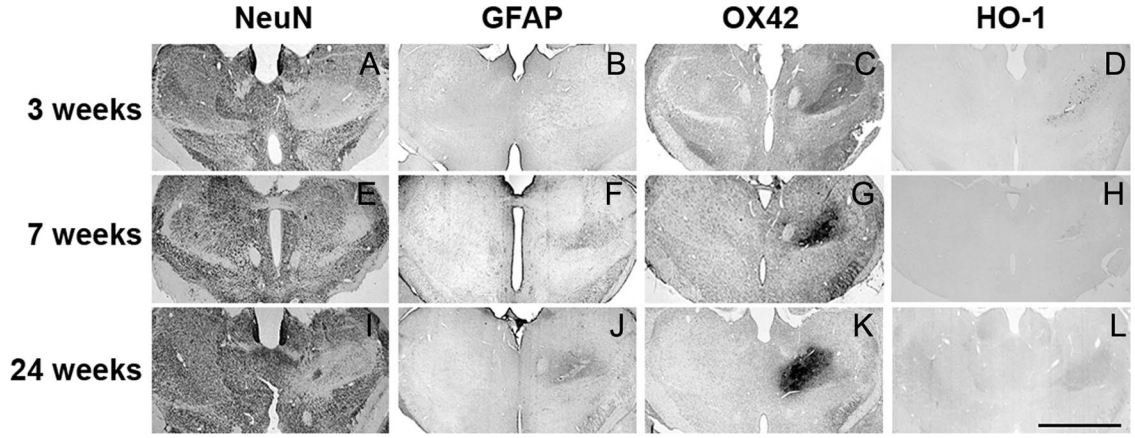

Figure 3. Chronological changes in thalamic expression of different cell population markers and inducible heme-oxigenase-1 after 1-hour MCAO. Four different markers (in columns) were tested at different time points after ischemia. Right thalamic nuclei corresponding to VPL and VPM showed neuronal loss detected as lack of NeuN immunostain at 3, 7 and 24 weeks (A, E, I). Glial reactivity and proliferation was tested with antibodies against GFAP (astrocytes: B, F, J) and OX42 (microglia: C, G, K). Marked GFAP expression was evident 7 weeks after ischemia (F). Twenty-four weeks after stroke, astrocytes were localized around the affected area, suggesting the formation of a glial scar (J). Strong microglial reactivity, detected by OX42 expression, was evident from the 3rd week and increased with time, probably attributable to cell proliferation (C, G, K). Heme-oxigenase-1 expression (D, H, L), detected in the thalamus 3 weeks after ischemia (D) disappeared with time (H, L), indicating a transient expression of this stress protein. Scale bar=2 mm.

Hyperintensities of T2-W images showed similar infarct extents as well as locations affected. For calculation of infarct volumes quantitative T2 maps were constructed from the multi-echo train for every time point studied from pre-MCAO to 6 months after occlusion. Statistical analysis of infarct volumes, based on T2 maps, was performed at 3 weeks when vasogenic edema as a confounding factor was already dissolved again. Infarct volumes did not show significant differences between groups (155±61, 134±46, 178±53 mm^3 for 3-, 7-, and 24-weeks group, respectively). T2 signal of infarcted areas was homogeneously high in caudate-putamen and parietal cortex from the third week after infarct to the last observation time point, indicating cystic transformation of the infarct core. Thalamic T2-W signal changes started the third week after stroke, showing a hyperintensity in thalamic nuclei ipsilateral to the lesion (Figure 2A). Contralateral thalamic nuclei did not show changes on T2-W signal intensity. Affected thalamic regions were identified as ventroposteromedial (VPM) and ventroposterolateral (VPL) nuclei by comparison with the Paxinos and Watson atlas.[17] Thalamic hyperintensity was not detected from 7 to 24 weeks after MCAO (Figure 2B and 2C). At the same experimental sessions 3D T2*-weighted sequences were acquired. Evolution of primary infarct showed irregular hypointensities in the infarct core according to T2*-W imaging, indicating microbleedings, reactive microglia, or infiltrating macrophages.

The same MR modalities showed patterns of evolution in the thalamus different from those in primarily affected cortical and striatal regions. Thalamic T2*-W images were apparently normal 3 weeks after the infarct (Figure 2D), whereas an intense hypointensity became evident 7 weeks after stroke (Figure 2E), persisting up to 24 weeks (Figure 2F). These regions with signal intensity decrease coincided with regions showing T2-W hyperintensity at 3 weeks after the ischemic insult (VPL and VPM).

Three weeks after ischemia neuronal loss was evident in VPL and VPM thalamic nuclei and remained until the end of the experiment (24 weeks; Figure 3A, 3E, and 3I). Glial reactivity was detectable from the third week on (Figure 3B and 3C). Astrocytic reaction was localized mainly around the VPL and VPM at 7 and 24 weeks after the infarct, forming an astrocytic scar (Figure 3F and 3J). Microglial reaction dramatically increased at 7 weeks (Figure 3G) compared to the expression at 3 weeks (Figure 3C). Microglial OX42 expression was still very important 24 weeks after stroke (Figure 3K). HO-1 expression in the ipsilateral thalamus was increased 3 weeks after MCAO compared to later time points, when only a small number of cells were detectable and these only barely (Figure 3D, 3H, and 3L). Cells expressing HO-1 at 3 weeks were identified by coexpression of microglial markers (Figure 4C).

Reactive microglia in the thalamus showed iron content at this time point (Figure 4B). Iron accumulation in the thalamus was evident from the third week after the onset of ischemia (Figure 4A). Iron was first clearly localized intracellularly (Figure 5A), whereas 7 weeks after infarct the iron showed a parenchymal distribution (Figure 5B). After 6 months iron was localized around thalamic structures similar to Alzheimer plaques (Figure 5C).

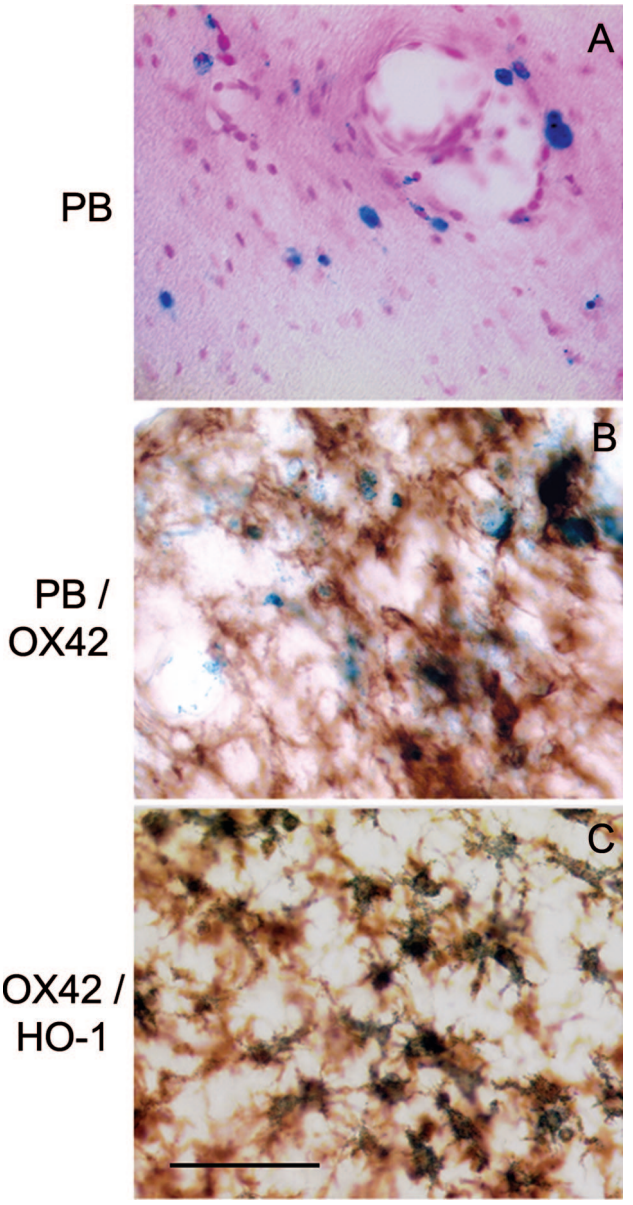

Figure 4. Thalamic ipsilateral detection of microglia (OX42), heme-oxigenase-1 (HO-1), and iron at 3 weeks after MCAO. Pearl Prussian blue iron detection with nuclear fast red counterstaining shows intracellular storage of iron in the thalamus (A). Iron was stored mainly in microglial cells at this time point, detected by double staining iron(blue)/OX42(brown) (B). HO-1 (black) was expressed by microglial (brown) cells in the thalamus 3 weeks after stroke (C). Scale bar=50 μm.

APP expression was localized as small dots in the VPL and VPM 3 weeks after ischemia. An increase in APP deposition was visually evident from week 7 after ischemia and was present until the end of the experiment (Figure 6A, 6B, and 6C). Double staining showed high density of microglial cells around the APP deposits (Figure 6D, 6E, and 6F).

Discussion

We have shown that high-resolution MRI is ideally suited to study long-term changes in brain regions remote from the primary infarct. We demonstrate here for the first time that T2*W-MRI permits to detect dynamics of iron accumulation

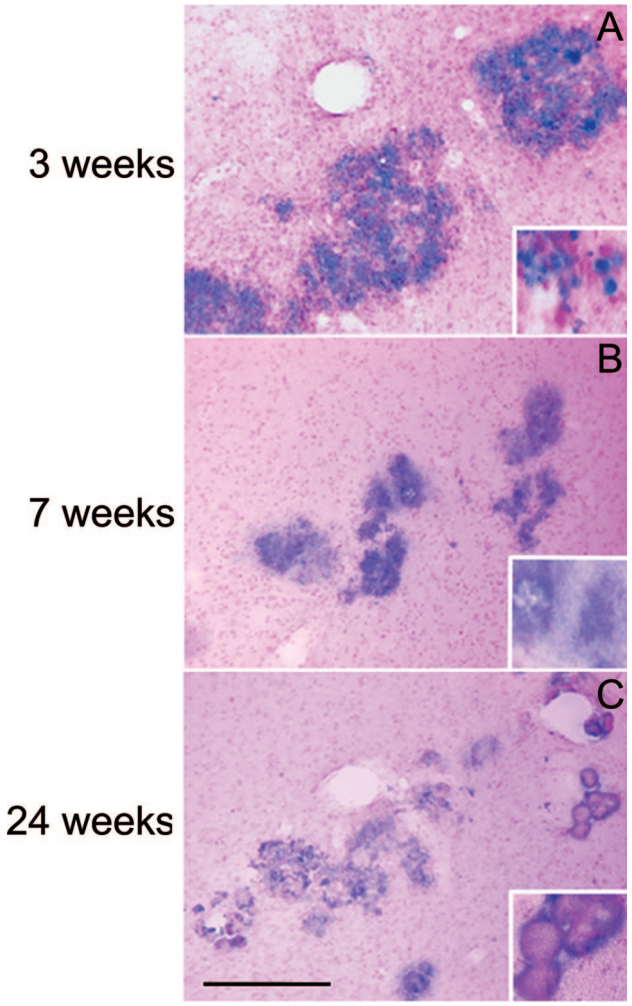

Figure 5. Iron accumulation in ipsilateral thalamic nuclei. Iron accumulates with a changing pattern. Three weeks after ischemia intracellular localization of iron is predominant (A), whereas 7 weeks after stroke iron is mainly distributed in the parenchyma (B). 24 weeks after ischemia iron tended to be distributed around plaque-like formations (C). Scale bar=200 μm.

in the thalamus, long after the onset of the ischemic episode. We have provided possible mechanisms that explain changes detected by MRI in the thalamus, including inflammation, oxidative stress, and microglial reactivity, among others.

One-hour occlusion of the MCA causes infarct formation in its supplying territory affecting ipsilateral basal ganglia and parietal cortex. These regions were affected in all animals in this study. But brain infarct is a dynamic process that includes anterograde and retrograde fiber degeneration of the axon, finally affecting parts remote from the primary infarct.[1] Neuronal secondary damage is a phenomenon that follows a long time course. MRI changes in remote areas have been reported in models of permanent MCA occlusion, indicating early alterations in thalamic nuclei and substantia nigra.[18,19] Using a model of transient MCA occlusion we were able to detect dynamic MRI changes in different brain regions, such as VPL and VPM thalamic nuclei, internal capsule, substantia nigra, and medial geniculate complex, among others. Thalamic neuronal death is detectable from 4 to 7 days after cortical lesion in mice and rats[5,20] and is delayed, appearing from 1 to 7 months after cortical lesion, in rabbits.[21] In a transient MCAO model in rats neuronal death in the thalamus was not detectable before 7 days, whereas a primary astrocytic and microglial reaction appeared already 3 days after the insult.[22] In our model we detected extensive neuronal death and glial reactivity, both events causing localized edema in the VPL and VPM nuclei 3 weeks after the ischemic insult. Increase in extracellular water content is detectable by increase in T2 values. Later permanent decrease in T2* values indicates a chronic accumulation of iron in the same thalamic nuclei.

Fetal cortical transplants reduce thalamic atrophy attributable to retrograde degeneration in thalamic nuclei ipsilateral to cortical lesions. This suggests that some trophic support is needed for the survival of thalamic neurons.[23] Altered levels of trophic factors causes degeneration of neurons and oligodendrocytes, both highly sensitive to such changes, inducing myelin degeneration.[24] This neuronal and oligodendrocytic degeneration leads to changes of connected regions, remote from the primary infarct, such as the thalamus and induces a delayed microglial reactivity and heme oxygenase expression.[25] Inducible heme-oxygenase (HO-1 or HSP-32) is a chaperone, hardly expressed under normal conditions but highly induced under oxidative stress,[26] degrading heme groups and generating biliverdin (a powerful antioxidant), CO, and iron.[14] We found transient expression of HO-1 at 3 weeks, at the same time that inflammation, delayed neuronal

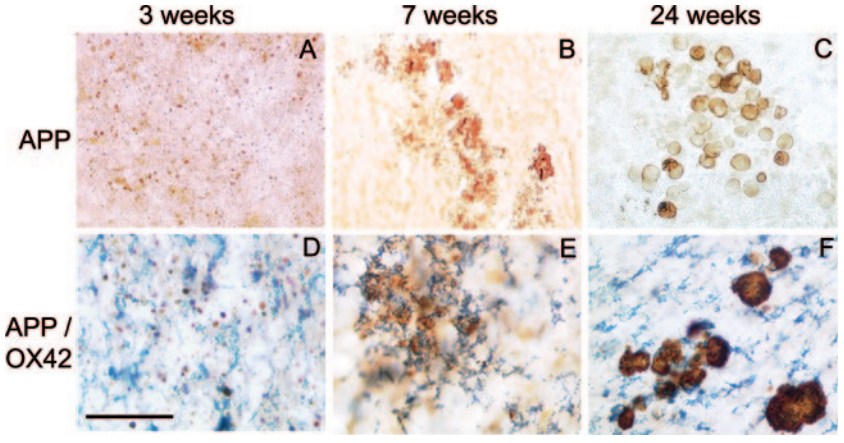

Figure 6. Amyloid precursor protein expression and localization. APP was accumulated first at synaptic terminals, appearing as small dots, 3 weeks after ischemia (A). Seven weeks after the infarct APP tended to aggregate (B) and form senile plaque-like aggregates (C) 24 weeks after stroke. At the same time points APP(brown)/OX42(blue) double staining showed microglial proliferation and reactivity around the APP aggregates (D, E, F). Scale bar=200 μm in A, B, C; 100 μm in D, E, F.

death, and microglial reaction took place. HO-1 expression has been used as an index of oxidative stress in neurodegenerative diseases such as Alzheimer disease[27] or amyotrophic lateral sclerosis,[28] suggesting that HO-1 could be an indicator of chronic oxidative stress. Different mechanisms try to neutralize damage caused by oxidative stress. The brain is particularly vulnerable to oxidative stress because of its high metabolic rate, using 20% of basal oxygen consumption. Inflammatory processes generate oxygen free radicals. The increase in HO-1 might contribute to an increased susceptibility to oxidative stress in elderly people.[29,30] Long-term expression of HO-1 is associated with Wallerian degeneration. HO-1 induction could also provide an index of microglial and macrophage stress response to injury.[26]

Mononuclear phagocyte lineage cells express ferritin. Light-chain ferritin, localized mainly in microglia in rats, is implicated in long-term iron storage.[26,31,32] HO-1 is found in both glial cells and neurons, whereas ferritin is only expressed by glia. Microglial cells have the capacity to sequester free iron, limiting iron mediated cell injury. Iron is potentially toxic, catalyzing hydroxyl radical formation via the Fenton reaction.[33]

Brain iron promotes protein oligomerization resulting in highly prevalent age-related proteinopathies such as Alzheimer disease (AD), Parkinson disease (PD), and Dementia with Leavy Bodies (DLB).[34,35] Protein accumulation is a widely observed phenomenon in neurodegenerative diseases. APP is an integral membrane protein expressed in many tissues and concentrated in the synapses of neurons. Amyloid beta (Aβ) is generated by APP proteolysis and is one of the primary components of amyloid plaques. APP production is present under normal conditions and at all ages but is increased under stress situation. APP is a marker of axonal degeneration, accumulates because of the disruption of axonal transport,[36] and is highly expressed by astrocytes in the ischemic border.[37] APP and Aβ chronic deposition have been reported in the thalamus after MCAO in rats[38] and humans.[39] There exists a balance between Aβ production and elimination acting through different mechanisms (microglial cells, astrocytes, insulin-degrading enzyme, among others). Thalamic APP accumulation could be the consequence of an increased production, or a decrease in elimination, or a combination of both mechanisms. We have found chronic APP expression, mainly by microglial cells from the third week after stroke on, in the thalamus ipsilateral to the infarct, in agreement with other reports.[38] APP accumulation shows a time-dependent varying pattern. At the earliest time point studied here APP was localized mainly as small dots, probably attributable to axonal degeneration. After 7 weeks APP adopted a plaque-like morphology with iron accumulation around the plaques. Alzheimer disease is linked to inflammation, with microglial and astrocytic increased reactivity, and metal biology, with presence of ions such as copper, zinc, and iron.[13,30] These metals accelerate Aβ peptide aggregation and enhance metal-catalyzed oxidative stress associated with amyloid plaque formation. The presence of an iron-responsive element (IRE) in the 5′UTR of the APP (APP 5′UTR) provided the first molecular biological support for the present model that APP of AD is a metalloprotein.[40] Neural toxicity is significantly attenuated after pretreatment of Aβ with iron-chelators, suggesting that the toxicity of Aβ is mediated via redox-active iron that enhances cellular oxidative stress.[41] Thus, iron can contribute to APP and Aβ toxicity and accumulation associated to stroke.

Summary

In the present investigation, we describe, for the first time, long-term changes detected by MRI in thalamic nuclei after MCAO in rats. These changes include neuronal loss and glial reactivity accompanied by edema, and followed by iron deposition, providing a mechanism that helps explain the observed temporal profile of T2*-weighted contrast on MRI.

Acknowledgments

Help with the immunohistochemical staining from Christiane Sprenger is gratefully acknowledged.

Sources of Funding

The investigation was supported by grants from the EU-FP6 program: DiMI (LSHB-CT-2005-512146), EMIL (LSHC-CT-2004-503569) and StemStroke (LSHB-CT-2006-037526).

Disclosures

None.

References

1. Fujie W, Kirino T, Tomukai N, Iwasawa T, Tamura A. Progressive shrinkage of the thalamus following middle cerebral artery occlusion in rats. *Stroke*. 1990;21:1485–1488.
2. Iizuka H, Sakatani K, Young W. Neuronal damage in the rat thalamus after cortical infarcts. *Stroke*. 1990;21:790–794.
3. Nordborg C, Johansson BB. Secondary thalamic lesions after ligation of the middle cerebral artery: an ultrastructural study. *Acta Neuropathol (Berl)*. 1996;91:61–66.
4. Garcia JH, Liu KF, Ye ZR, Gutierrez JA. Incomplete infarct and delayed neuronal death after transient middle cerebral artery occlusion in rats. *Stroke*. 1997;28:2303–2309.
5. Ross DT, Ebner FF. Thalamic retrograde degeneration following cortical injury: An excitotoxic process? *Neuroscience*. 1990;35:525–550.
6. Domercq M, Etxebarria E, Perez-Sanmartin A, Matute C. Excitotoxic oligodendrocyte death and axonal damage induced by glutamate transporter inhibition. *Glia*. 2005;52:36–46.
7. Johnston MV. Excitotoxicity in perinatal brain injury. *Brain Pathol*. 2005;15:234–240.
8. Pesini P, Copp J, Wong H, Walsh JH, Grant G, Hökfelt T. An immunohistochemical marker for Wallerian degeneration of fibers in the central and peripheral nervous system. *Brain Res*. 1999;828:41–59.
9. Myers R, Manjil LG, Franckoviak RS, Cremer JE. [3H]PK11195 and the localisation of secondary thalamic lesion following focal ischemia in the rat motor cortex. *Neurosci Lett*. 1991;133:20–24.
10. Pappata S, Levasseur M, Gunn R, Myers R, Crouzel C, Syrota A, Jones T, Kreutzberg G, Banati RB. Thalamic microglial activation in ischemic stroke detected in vivo by PET and [11C]PK11195. *Neurology*. 2000;55:1052–1054.
11. Carbonell T, Rama R. Iron, oxidative stress and early neurological deterioration in ischemic stroke. *Curr Med Chem*. 2007;14:857–874.
12. Khong PL, Zhou LJ, Ooi GC, Chung BH, Cheung RT, Wong CN. The evaluation of Walleriann degeneration in chronic paediatric middle cerebral artery infarction using diffusion tensor MR imaging. *Cerebrovasc Dis*. 2004;18:240–247.
13. Maynard CJ, Bush AI, Masters CL, Cappai R, Qiao-Xin L. Metals and amyloid-beta in Alzheimer's disease. *Int J Exper Pathol*. 2005;86:147–159.
14. Koistinaho J, Miettinen S, Keinänen R, Vartiainen N, Roivainen R, Laitinen JT. Long-term induction of haem oxygenase-1 (HSP-32) in astrocytes and microglia following transient focal brain ischaemia in the rat. *Eur J Neurosci*. 1996;8:2265–2272.

15. Schallert T, Whishaw IQ. Bilateral cutaneous stimulation of the somatosensory system in hemidecorticate rats. *Behav Neurosci*. 1984;98:518–540.
16. Wegener S, Weber R, Ramos-Cabrer P, Uhlenküken U, Wiedermann D, Kandal K, Villringer A, Hoehn M. Subcortical lesions after transient thread occlusion in the rat: T2-weighted magnetic resonance imaging findings without corresponding sensorimotor deficits. *J Magn Reson Imaging*. 2005;21:340–346.
17. Paxinos G, Wattson C. *The Rat Brain in Stereotaxic Coordinates*. IV ed. Academic Press, San Diego. 1998;
18. Nakane M, Tamuar A, Nagaoka T, Hirakawa K. MR detection of secondary changes remote from ischemia: preliminary observations after occlusion of the middle cerebral artery in rats. *Am J Neuroradiol*. 1997;18:945–950.
19. Abe O, Nakane M, Aoki S, Hayashi N, Masumoto T, Kunimatsu A, Mori H, Tamura A, Ohmoto K. MR imaging of postischemic neuronal death in the substantia nigra and thalamus following middle cerebral artery occlusion in rats. *NMR Biomed*. 2003;16:152–159.
20. Sorensen JC, Dalmau I, Zimmer J, Finsen B. Microglial reactions to retrograde degeneration of tracer-identified thalamic neurons after frontal sensorimotor cortex lesions in adult rats. *Exper Brain Res*. 1996;112:203–212.
21. Matthews MA. Death of the central neuron: an electron microscopic study of thalamic retrograde degeneration following cortical ablation. *J Neurocytol*. 1973;2:262–288.
22. Hermann DM, Mies G, Hata R. Microglial and astrocytic reactions prior to onset of thalamic cell death after traumatic lesion of the rat sensorimotor cortex. *Acta Neuropathologica (Berlin)*. 2000;99:147–153.
23. Sharp FR, Gonzalez MF. Fetal cortical transplants ameliorate thalamic atrophy ipsilateral to neonatal frontal cortex lesions. *Neurosci Lett*. 1986;71:247–251.
24. Drojdahl N, Fenegr C, Nielsen HH, Owens T, Finsen B. Dynamics of oligodendrocyte responses to anterograde axonal (Wallerian)and terminal degeneration in normal and TNF-transgenic mice. *J Neurosci Res*. 2004;75:203–217.
25. Bidmon HJ, Emde B, Oermann E, Kubitz R, Witte OW, Zilles K. Heme oxygenase-1(HSP-32) induction in neurons and glial cells of cerebral regions and its relation to iron accumulation after focal cortical photothrombosis. *Exper Neurol*. 2001;168:1–22.
26. Mautes AE, Bergeron. M, Sharp FR, Panter SS, Weinzierl M, Guenther K, Noble LJ. Sustained induction of heme oxygenase-1 in the traumatized spinal cord. *Exper Neurol*. 2000;166:254–265.
27. Schipper HM, Bennet DA, Liberman A, Bienias JL, Schneider JA, Kelly J, Arvanitakis Z. Glial heme oxygenase-1 expression in Alzheimer's disease and mild cognitive impairment. *Neurobiol Aging*. 2006;27:252–261.
28. Dwyer BE, Lu SY, Nishimura RN. Heme oxygenase in the experimental ALS mouse. *Exper Neurol*. 1998;150:206–212.
29. Hirose W, Ikematsu K, Tsuda R. Age-associated increases in heme oxygenase-1 and ferritin immunoreactivity in the autopsied brain. *Legal Med (Tokyo)*. 2003;5:s360–s366.
30. Zecca L, Youdim MB, Riederer P, Connor JR, Crichton RR. Iron, brain aging and neurodegenerative disorders. *Nat Rev*. 2004;5:863–873.
31. Connor JR, Boeshore KL, Benkovic SA, Menzies SL. Isoforms of ferritin have a specific cellular distribution in the brain. *J Neurosci Res*. 1994;37:461–465.
32. Melhase J, Gieche J, Widmer R, Grune T. Ferritin levels in microglia depend upon activation: Modulation by reactive oxygen species. *Biochem Biophys Acta*. 2006;1763:854–859.
33. Crichton RR, Wilmert S, Legssyer R, Ward RJ. Molecular and cellular mechanisms of iron homeostasis and toxicity in mammalian cells. *J Inorg Biochem*. 2002;91:9–18.
34. Bush AI. The metallobiology of Alzheimer's disease. *Trends Neurosci*. 2003;26:207–214.
35. Bartzokis G, Tishler TA, Lu PH, Villablanca P, Altshuler LL, Carter M, Huang D, Edwards N, Mintz J. Brain ferritin iron may influence age- and gender-related risks of neurodegeneration. *Neurobiol Aging*. 2007;28:414–423.
36. Smith DH, Uryu K, Saatman KE, Trojanowski JQ, McIntosh TK. Protein accumulation in traumatic brain injury. *Neuromol Med*. 2003;4:59–72.
37. Popa-Wagner A, Schroder E, Walker LC, Kessler C. beta-amyloid precursor protein and ss-amyloid peptide immunoreactivity in the rat brain after middle cerebral artery occlusion: effect of age. *Stroke*. 1998;29:2196–2202.
38. Van Groen T, Puurunen K, Mäki HM, Sivenius J, Jolkkonen J. Transformation of diffuse (beta)-amyloid precursor protein and (beta)-amyloid deposits to plaques in the thalamus after transient occlusion of the middle cerebral artery in rats. *Stroke*. 2005;36:1551–1556.
39. Aho L, Jolkkonen J, Alafuzoff I. beta-amyloid aggregation in human brains with cerebrovascular lesions. *Stroke*. 2006;37:2940–2945.
40. Rogers JT, Randall JD, Cahill CM, Eder PS, Huang X, Gunshin H, Leiter L, McPhee J, Sarang SS, Utsuki T, Greig NH, Lahiri DK, Tanzi RE, Bush AI, Giordano T, Gullans SR. An iron-responsive element type II in the 5′-untranslated region of the Alzheimer's amyloid precursor protein transcript. *J Biol Chem*. 2002;277:45518–45528.
41. Rottkamp CA, Raina AK, Zhu X, Gaier E, Bush AI, Atwood CS, Chevion M, Perry G, Smith MA. Redox-active iron mediates amyloid-b toxicity. *Free Rad Biol Med*. 2001;30:447–450.